GI_Forum 2018, Issue.1
Page: 90 - 104
Full Paper
Corresponding Author:
kglock@fzi.de
DOI: 10.1553/giscience2018_01_s90

Micro Rapid Mapping: Automatic UAV-based Remote Sensing for Chemical Emergencies

Katharina Glock[1], Anne Meyer[1], Bodo Bernsdorf[2] and Sascha Woditsch[2]

1 FZI Forschungszentrum Informatik am Karlsruher Institut für Technologie, Germany
2 EFTAS Fernerkundung Technologietransfer GmbH, Münster, Germany

Abstract

In chemical emergencies, response units rely on the speedy provision of detailed information about the area affected by potentially hazardous substances in order to decide on efficient response actions. Unmanned Aerial Vehicles (UAVs) equipped with remote sensing equipment offer a flexible way of providing this information. Hence, these systems are becoming more and more interesting for firefighters and plant operators alike. Although having to actively control the UAVs makes high demands on the response squad in an already stressful situation, cyber-physical systems that allow the automatic deployment of UAVs have rarely been studied to date.
We present and evaluate a system for planning UAV missions in emergency situations. We propose two different planning algorithms: (1) a mapping approach for covering the entire target area; (2) an algorithm that selects sensing locations across a wide area in order to allow quicker exploration. We verify the applicability in an extensive simulative study and demonstrate the information gain achieved, as well as the remaining uncertainty, after a flight, about the spatial phenomenon observed.

Keywords:

micro rapid mapping, mission planning, correlated orienteering, QGIS, situational awareness

1 Introduction

Chemical emergencies resulting from fires or accidents often involve large contaminated areas and hazardous substances that may be invisible or scentless. This poses a problem for emergency response and relief units who require reliable information about the affected area as well as the chemicals involved. This information allows the emergency services to decide on the appropriate protective equipment, to plan the warning and evacuation of the population, and to coordinate the effective deployment of response units.

Remote sensing technologies are a popular means for providing up-to-date information within a short time after an incident. Arguably the best-known examples of such technologies are satellite-based systems such as the Copernicus Emergency Management

Service (see. e.g. Guzzetti et al., 2012; European Parliament, 2017). The objective of the Copernicus programme is to provide up-to-date information within several hours or days after large-scale disasters. However, for the majority of emergencies faced by firefighters and other response units, this delay is prohibitively high. For these applications, small Unmanned Aerial Vehicles (UAVs) are attracting increased interest. Compared to satellite-based applications, they are more flexible and can be launched with minimal delay after an incident. As they cover much smaller areas than a satellite-based system and the mission duration is limited to minutes or hours, we call this approach 'micro rapid mapping'.

In this paper, we present a mission-planning system that enables response units to deploy UAVs automatically after an incident. Depending on the size of the affected area and the available flight time of the UAV, this system plans surveillance missions that either ensure complete coverage of the target area or include selected sensing locations in order to quickly estimate the extent of the contamination. We evaluate the proposed algorithms in an extensive simulative study and analyse the information gain, as well as the remaining uncertainty about the observed phenomenon, in order to demonstrate the applicability of the mission-planning system.

2 Emergency Surveillance Using UAVs

The surveillance planning problem discussed here was studied as part of a research project that seeks to develop new technologies for the effective use of UAVs in the context of firefighting. The success of such a cyber-physical system depends on three things:

(1) The availability of appropriate hardware and equipment, i.e. vehicles with sufficient speed, range and robustness for practical applications;
(2) Remote sensing technologies and data processing tools fit for the mission in question, i.e. sensors able to detect hazardous gases or fire pockets;
(3) Software supporting the immediate and automatic deployment of UAVs requiring as little manual oversight as possible.

Significant progress has been made in all three areas in recent years. For example, among the currently available UAV systems are multicopters that are able to transport sensors and processing equipment with a total weight of up to 5 kg for around 20 to 30 minutes. This is sufficient for most scenarios that firefighters face. The available sensing devices include thermal and hyperspectral sensors as well as conventional video cameras. Lightweight thermal cameras allow the monitoring of fires and the detection of people. Other thermal imagining systems are able to identify specific substances, such as carbon monoxide or methane (FLIR, 2017). UAV-based hyperspectral imaging systems have already found widespread use in agriculture (Zhang & Kovacs, 2012; Mulla, 2013) and are becoming more relevant for other applications. In the BigGIS research project, for example, we studied the potential of these cameras for detecting substances in smoke clouds. Figure 1 gives an example from a preliminary test in which a UAV surveyed an artificially created smoke cloud blended with chlorophyll. This technology is particularly interesting for the chemical industry, where prior knowledge about potential contaminants is available. A UAV equipped with an appropriate sensor provides a flexible tool for a wide range of hazardous gases.

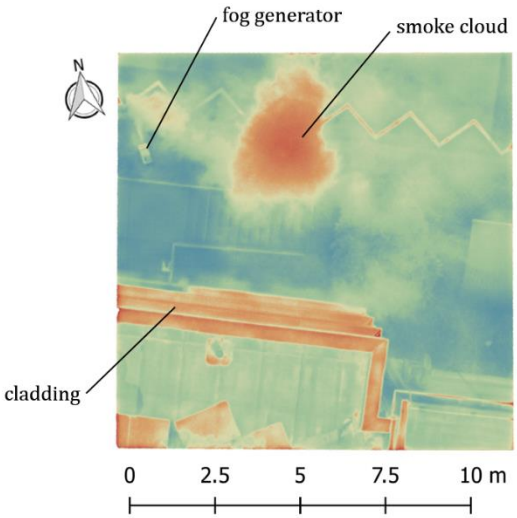

Figure 1: Section of a georeferenced hyperspectral image of an artificially created smoke cloud blended with chlorophyll

UAV mission-planning tools that relieve human decision-makers have received less attention. Usually, a UAV's missions are planned either ad-hoc by a human operator, based on a live video stream, or by using a planning tool that focuses on the complete coverage of a designated target area (see e.g. Galceran & Carreras, 2013). In this paper, we present an interactive tool that supports a human decision-maker in this task. An interface in the form of a QGIS plugin (QGIS Development Team, 2017) allows the user to specify the area of interest, flight altitude and other parameters. Figure 2 shows a screenshot of this plugin with a specified target area and mission-planning parameters. Using this information, the application then computes a two-stage flight plan. In the first stage, the UAV provides an initial survey image of the entire target area at high altitude. This serves as a preliminary indication of the situation for the human decision-maker. In the second-stage, high-resolution images are provided at low altitude. Here, the user can choose between two planning variants:

(1) If the time available for executing the flight is sufficient, the UAV can map the entire target area. In this case, the system computes a vehicle route with minimum resource requirements, resulting in a regular pattern such as the one depicted in Figure 2.
(2) If complete coverage is not possible, the target area is divided into a regular grid of potential target points. The tool plans a mission by selecting a subset of target locations that the UAV visits during its flight. In order to provide the user with particularly relevant information, priorities within the target area are taken into account when deciding on this subset of targets. In the context considered here, these priorities are determined based on the initial survey image. Specifically, the areas where an initial analysis of the survey images indicates a high likelihood of hazardous substances being present are of particular interest for the decision-maker. These areas are therefore prioritized for the detailed flight. High-resolution images can then

confirm the assessment, detect erroneous measurements or classifications, and accurately determine the nature and extent of the contamination.

In the context of firefighting, the command vehicle is equipped with a computer, ground station and radio transceiver, thus allowing the transmission of high-resolution images during the flight. The data is then immediately available for detecting substances. Up-to-date images can be visualized by the user via the same QGIS tool, thus eliminating the overheads necessary for operating distinct planning and visualization systems.

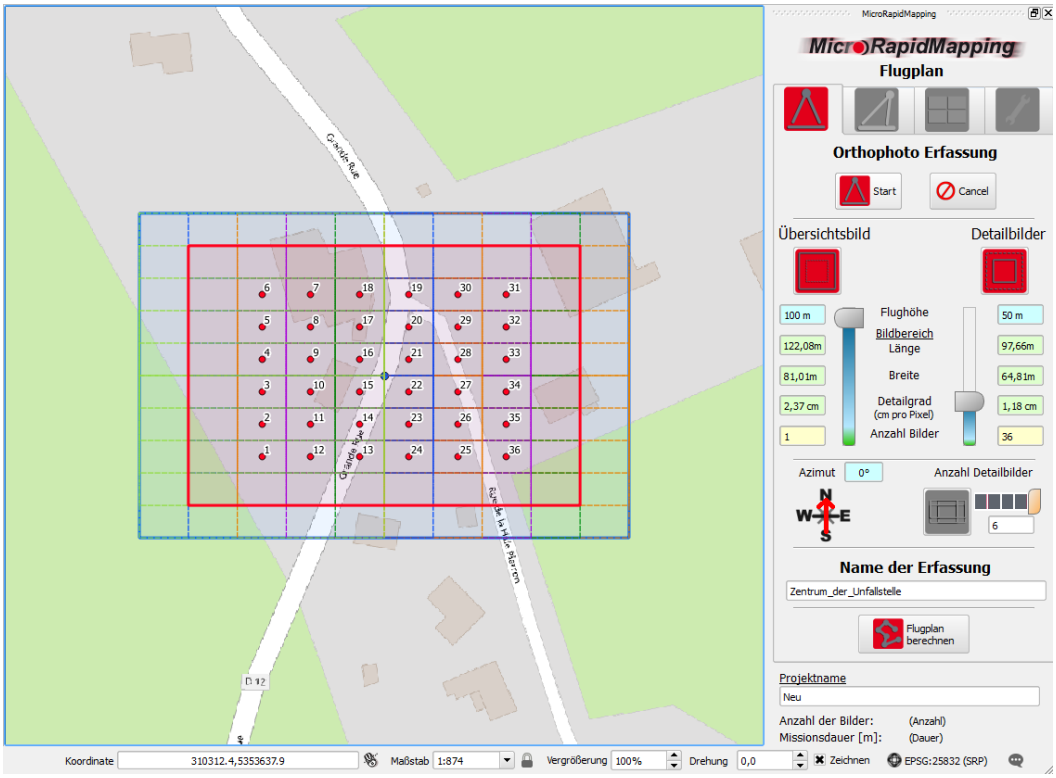

Figure 2: Interface for planning UAV missions in QGIS. The flight plan indicates target points (red) as well as the area covered. Flight altitude, number of pictures and camera specifications are set on the right-hand side.

3 Mission Planning

In this section, we present in more detail the two planning alternatives for micro rapid mapping. Both mission-planning approaches determine a sequence of discrete waypoints, each of which represents the centre of one image taken by the UAV. The corresponding missions are communicated to the UAV, which can then automatically traverse the target region.

Complete Coverage

If the complete coverage of the target area is possible, the mission-planning algorithm determines a covering path of the shortest length possible. In this case, the UAV traverses the area following a regular pattern (see e.g. Figure 2). Figure 3 gives the algorithm for computing the target locations in order. The algorithm can account for overlap requirements between adjacent images, which facilitates image post-processing. Different overlaps can be specified for forward and side overlap, i.e. overlap in the direction of the route and overlap in the lateral direction.

Input: target area bounding box $\{(x_l, y_l), (x_u, y_u)\}$ defined by lower-left and upper-right coordinates, image side length k, overlap in the direction of the flight r_l and orthogonal to the direction of the flight r_w

Return: ordered sequence of target locations $P = [(x_0, y_0), \dots, (x_n, y_n)]$

Number of images along each axis: $n_x = \text{ceil}(\frac{x_u - x_l}{k \cdot r_l}), n_y = \text{ceil}(\frac{y_u - y_l}{k \cdot r_w})$

Total number of target images $n = n_x \cdot n_y$

Determine first location (x_0, y_0) with $x_0 = x_l + 0.5k \cdot r_l,\ \ y_0 = y_l + 0.5k \cdot r_w$

Initialize line count $l = 1$, target point index $i = 1$

Do

  If $i \bmod n_x = 0$ **then**

    $l = l + 1$ (▷ continue with the next line of target points)

    $y_i = y_{i-1} + 0.5k \cdot r_w$

  Else $y_i = y_{i-1}$

  If $l > n_y$ **then break** (▷ stop computation: entire region is covered)

  If $l \bmod 2 = 0$ **then** $x_i = x_{i-1} - 0.5k \cdot r_l$

  Else $x_i = x_{i-1} + 0.5k \cdot r_l$

  $i = i + 1$

Figure 3: Mission-planning algorithm for complete coverage

Selective Mission Planning

If complete coverage is not possible, the planning problem consists in providing as much useful information to the human decision-maker as possible while respecting the limited

flight time and range. This planning problem is a variant of the orienteering problem (see e.g. Gunawan et al., 2016), which consists in selecting a subset of targets to visit and determining the order in which to visit them.

The Orienteering-Problem Model

We can formally define the underlying planning problem as follows: we consider a set of candidate target locations $= \{v_0, \dots, v_k\}$, each of which is associated with a reward value $u_i > 0$. In our case, rewards represent the reflectance in the initial survey image at relevant wavelengths. The reward is obtained when a sensing location is included in the UAV's flightpath. Hence, areas that are more likely to be affected by critical substances are prioritized when planning the UAV mission. Travel between distinct targets is associated with a non-negative travel time τ_{ij}, and surveying a target location requires a fixed time τ_{fix}. The UAV has a maximum allowed travel time budget B. The objective is to determine a path P through a subset of the candidate waypoints in V such that maximum travel time is not exceeded and the total information gain is maximal.

Objective Function

A crucial aspect of this orienteering problem is how the notion of 'information gain' can be operationalized for planning UAV routes. In the case of emergency surveillance, the selected target locations that make up the path should have a high priority – i.e., in the case of a chemical emergency, they need to be associated with potentially high concentrations of contaminants. Furthermore, we want to exploit spatial correlations in order to increase information gain. Following Tobler's first law of geography, we can assume that observations at sensing locations in close proximity to one another are similar. Knowing that, we therefore want to select sensing locations that are well distributed across the target area rather than focusing solely on hotspots. In this way, we can achieve a reliable idea of the true extent of the observed phenomenon.

Yu et al. (2014) proposed a quadratic objective function that balances priorities and spatial dependencies. Specifically, they explicitly include partial utilities $\sum w_{ji} u_i$ for targets that are close to the UAV's flightpath, but not visited by the UAV. Here, $w_{ij} \in [0,1]$ is a weighting factor representing the strength of the correlation between $v_i, v_j \in V$. Explicitly modelling these partial utilities reduces the marginal benefit of sensing locations if other observations are made nearby. Hence, the model encourages a broader exploration of the target area.

In this study, we define weighting factors such that they decrease with distance. We model information gain using a generalized formulation of the model proposed by Yu et al. (2014). For this formulation, we introduce additional binary variables $z_i, v_i \in V$ with $z_i = 1$ if $v_i \in P$ and $z_i = 0$ otherwise. The resulting metric is:

$$I(P) = \sum_{v_i \in V} \left(z_i u_i + (1 - z_i) \min \left\{ \sum_{v_j \in V} w_{ji} u_i (z_j - z_i) \right\} \right) \quad \text{(eq. 1)}$$

In the remainder of this paper, we refer to the problem of maximizing $I(P)$ as the Correlated Orienteering Problem (CorOP).

Local Search

As a generalization of the well-known Travelling Salesman Problem, the CorOP is NP-hard (Lenstra & Kan, 1981). We solve the planning problem using the Adaptive Large Neighbourhood Search proposed by Pisinger & Ropke (2007) rather than attempting to find an exact solution. This algorithm has been shown to provide solutions of high quality with short computation times, which is of particular importance for the application considered here.

In Figures 4 and 5, we give the pseudocode for two key components of the algorithm: the construction heuristic in Figure 4 builds a vehicle path by iteratively inserting targets such that they maximize some utility metric $util(v)$. This metric may, for example, represent the direct utility u_v or the marginal utility that can be achieved by adding a target location v; i.e. $util(v) = I(P_{partial} \cup v) - I(P_{partial})$ where $P_{partial}$ is a partially constructed vehicle path. All targets are inserted in the emerging UAV path such that the necessary detour is minimal.

Input: partially constructed path $P_{partial}$
Return: ordered sequence of target locations $P = [(x_0, y_0), \dots, (x_n, y_n)]$
1: Initialize utility metric *util(v)*
2: **While** $cost(P_{partial}) < B$
3: Select location $v \in V \backslash P_{partial}$ such that $v = \text{argmax}_{v \in V \backslash P_{partial}}\, util(v)$
4: Add v to path $P_{partial}$ at the minimum detour position

Figure 4: Construction heuristic for iteratively building vehicle routes

The algorithm in Figure 5 depicts the Large Neighbourhood Search approach in which we embedded this construction heuristic. This heuristic modifies a solution by iteratively destroying and rebuilding parts of it in order to improve its total utility. The destruction operator removes some of the selected sensing locations from the vehicle's planned flightpath in the current solution. Starting with the resulting partial solution, the construction heuristic then rebuilds a full UAV path. Using different utility metrics in this construction phase allows the rapid diversification of solutions in order to improve their objective value, and hence their utility. Finally, an acceptance criterion determines whether a solution is accepted or not. In our algorithm, improving solutions are always accepted, whereas solutions of decreasing utility are accepted with a probability that increases with the number of non-improving iterations in order to avoid or leave local minima.

Input: set of candidate targets locations $V = \{v_1, v_2, \dots, v_k\}$, vector of associated utilities $u_i > 0 \; \forall \; v_i \in V$, matrix of weights $w_{ij} \in [0,1] \; \forall \; v_i, v_j \in V$
Return: ordered sequence of target locations $P_{best} = [(x_0, y_0), \dots, (x_n, y_n)]$
Construct starting solution P_{start} using the construction heuristic in Figure 4

Initialize $P_{current} = P_{start}, P_{best} = P_{start}, i = 0$

While i is less than the maximum number of iterations

$$P_{part} = destroy(P_{current})$$

$$P_{new} = construct(P_{part})$$

If $I(P_{new}) > I(P_{best})$ **then** $P_{best} = P_{new}, P_{current} = P_{new}$

Else if $accept(P_{new})$ **then** $P_{current} = P_{new}$

$$i = i + 1$$

Figure 5: Large Neighbourhood Search approach

4 Simulative Study

We verify the applicability of the proposed mission-planning system by using an extensive simulative study. As this study focuses on applications in firefighting, we specifically address incidents where the affected area is too large to easily develop or maintain situational awareness, e.g. major fires in industrial or residential areas. Note that we do not consider large-scale disasters, which are at the centre of the Copernicus Rapid Mapping programme. We therefore propose three scenarios that differ in terms of the size of the target region. In the first scenario, we consider a target area of 750 m x 750 m, i.e. approximately 0.56 km². This is approximately the maximum area that a single UAV can cover within its maximum flight time. The other two scenarios consider larger areas, of 1 km² and 1.56 km². These scenarios serve to show the effectiveness of UAV missions in target areas that cannot be covered in their entirety.

Table 1 indicates all relevant vehicle and camera specifications for this use case. The parameters used are feasible for technologies currently available on the market, for example an AiD-MC8 Octocopter[1] equipped with a Cubert S185 FireflEYE SE hyperspectral camera[2].

The target ground resolution is determined following Johnson's criteria, a system of methods and indicators used for predicting the ability of a human observer to distinguish between objects depending on the number of pixels available. This system thus provides a rough approximation of an operational resolution. For example, approximately 10 pixels are required to detect a person, and approximately 50 to 80 pixels to identify one (i.e. to

[1] https://www.aidrones.de/english/drone-systems/octocopter-mc8/
[2] http://cubert-gmbh.com/product/uhd-185-firefly/

distinguish a person from other objects) (Petrides et al., 2017). Based on these criteria, we can assume that a ground resolution of 5 cm is sufficient for detecting a human individual in images provided by a UAV. Given the camera specifications and this target resolution, this implies a flight altitude of 70 m for the detailed survey pictures. Each of the resulting images then covers an area with a side length of 50 m.

Before planning UAV routes, we separate the target areas into discrete target points, each of which represents the centre of a single image taken by the UAV. These target points are 50 m apart. The target area of scenario 1 therefore contains 15 x 15 = 225 candidate target points; scenario 3 includes 25 x 25 = 625 target points.

Table 1: Vehicle and sensor configurations and target area size for the simulative study

UAV system	Max. flight time	5 to 30 minutes
	Cruise speed	10 m/s
	Acceleration	3 m/s^2
Sensor system	Camera resolution	1MP
	Focal length	12 mm
	Target ground resolution	5 cm
	Resulting flight altitude	70 m
Target area	Scenario 1	750 m x 750 m
	Scenario 2	1,000 m x 1,000 m
	Scenario 3	1,250 m x 1,250 m

For each scenario, we created five synthetic, autocorrelated random fields using the gstat package (Pebesma et al., 2017). The simulated values varied between 0 and 100. Figure 6 gives an example of the semivariogram describing the generated data and one realization of such a random field. Maximum flight durations vary between 5 and 30 minutes, resulting in a total of 30 instances per scenario.

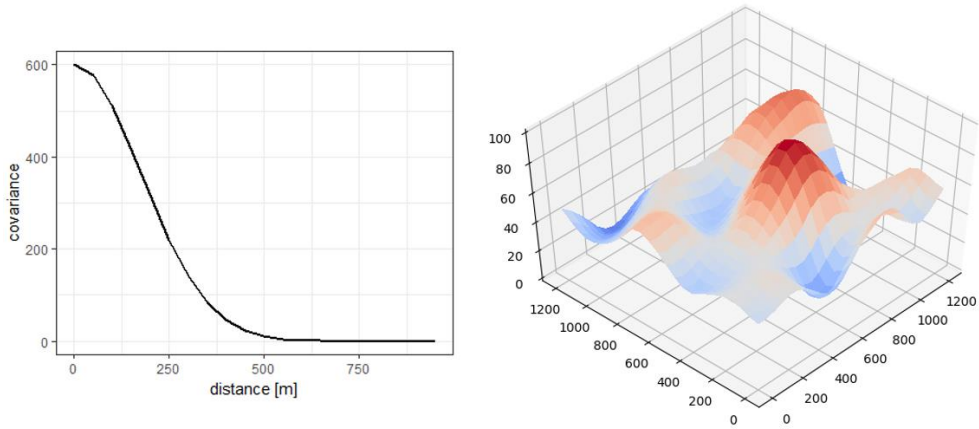

Figure 6: Generation of synthetic test data. Left: Gaussian kernel used for spatial simulation. Right: Resulting realization of a spatially autocorrelated random field.

5 Results

The objective of the simulative study was to demonstrate the applicability of an automatic surveillance approach in an emergency. We therefore applied the proposed planning algorithms to the test instances derived in Section 4. In this section, we evaluate the algorithms' results focusing on two aspects that are relevant for potential users of such a surveillance system: the spatial coverage achieved and the information gain achieved.

Spatial Coverage

For a human decision-maker, information about the spatial distribution of contaminants across an entire target area is arguably the most important information. We therefore evaluated the area covered for both mission-planning approaches proposed in Section 4.

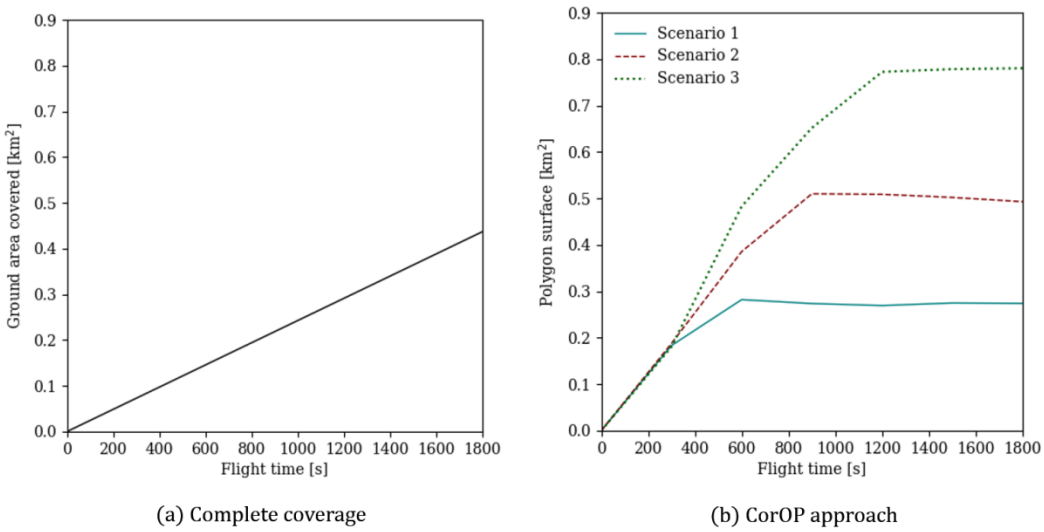

Figure 7: Achievable coverage depending on the flight time for both planning algorithms.

The results are summarized in Figure 7. The graph on the left-hand side indicates the maximum area that a UAV can cover in its entirety as a function of the available flight time. In order to provide an unbiased comparison with regard to the orienteering-problem formulation, this evaluation disregards the overlap that may be required for a mapping flight. Given a flight time of 1,800 seconds, a single UAV can cover only around 0.5 km² this way. Obviously, complete surveillance is realistic in cases of small affected regions, but quickly becomes impractical for larger target areas or when there is a tight restriction on maximum flight times.

We apply the CorOP approach only when complete coverage is impossible, i.e. when the potentially affected area after an incident exceeds the maximum coverable area. In this case, we seek to evaluate whether the UAV route traverses sufficiently large parts of the target

area. To do this, we evaluate the size of the polygon formed by a UAV route P consisting of n waypoints:

$$A(P) = 0.5 \sum_{i=0}^{n-1} (x_i y_{i+1} - x_{i+1} y_i)$$

We present the results in Figure 7 (b). We can see that polygon size quickly increases with flight time. For all scenarios, it converges to a value that corresponds to roughly half the target area size: for the smallest scenario, the average polygon area converges to 0.3 km², whereas for a target region of 1.6 km², this value is as high as 0.8 km². The evaluation shows, furthermore, that this threshold can be attained within a maximum flight time that is well below the time required for full coverage. For the target region size of 0.6 km², we reach the threshold value within 700 seconds. For the larger scenarios, the flight time increases to around 1,200 to 1,300 seconds. Hence, we can conclude that the planning approach selects sensing locations that are well distributed across the target area. As we demonstrate in the next section, this means that we can achieve a reliable estimate for the phenomenon of interest within a short time span.

Information Gain

In this section, we evaluate whether the survey flights yield reliable information for the human decision-maker, even though the UAV only visits a subset of all potential target locations. In particular, we evaluate solutions in a post-processing step in which the information gained at these locations is used for interpolating the underlying spatial phenomenon. Information gain can then be measured as the accuracy of the prediction and the uncertainty remaining within the process.

To do this, we combine the information about the spatial distribution with the samples provided by the UAV at the selected target points. We use this data to compute an interpolation of the remaining (i.e. unsurveyed) field via Gaussian Process regression. The better this interpolation is, the better we consider the selected set of sampling locations to be. We evaluate the quality of the interpolation based on (1) the root-mean-square error (RMSE) made with regard to the initial data, (2) the resulting prediction error variance, and (3) the mean error, i.e. a potential bias in the prediction.

Figure 8 gives an example of this evaluation. Here, we compare the information gain achieved by three flights planned for the same target area, of three different maximum flight durations (300 seconds, 600 seconds and 900 seconds respectively). The target area is the same one as in Figure 6. The planned UAV missions are indicated in row (a). We then give the interpolation for the entire target region based on the sampling locations selected for the flight. The bottom row indicates the prediction error variances associated with this interpolation. In order to enable an unbiased comparison of the different approaches and the information gain achieved, we assume that all samples are made without error and that the information about the underlying spatial phenomenon is accurate, i.e. that its covariance is known.

The results show that, given a flight time limited to 300 seconds, the UAV quickly moves to the centre of the image and then turns towards a region associated with high-priority values. The interpolation achieved is accurate for this region but lacking in other parts of the target area. Consequently, the error variance for these areas is high. In comparison, the longer flight times of 600 and 900 seconds provide fairly reliable estimates of the entire random field.

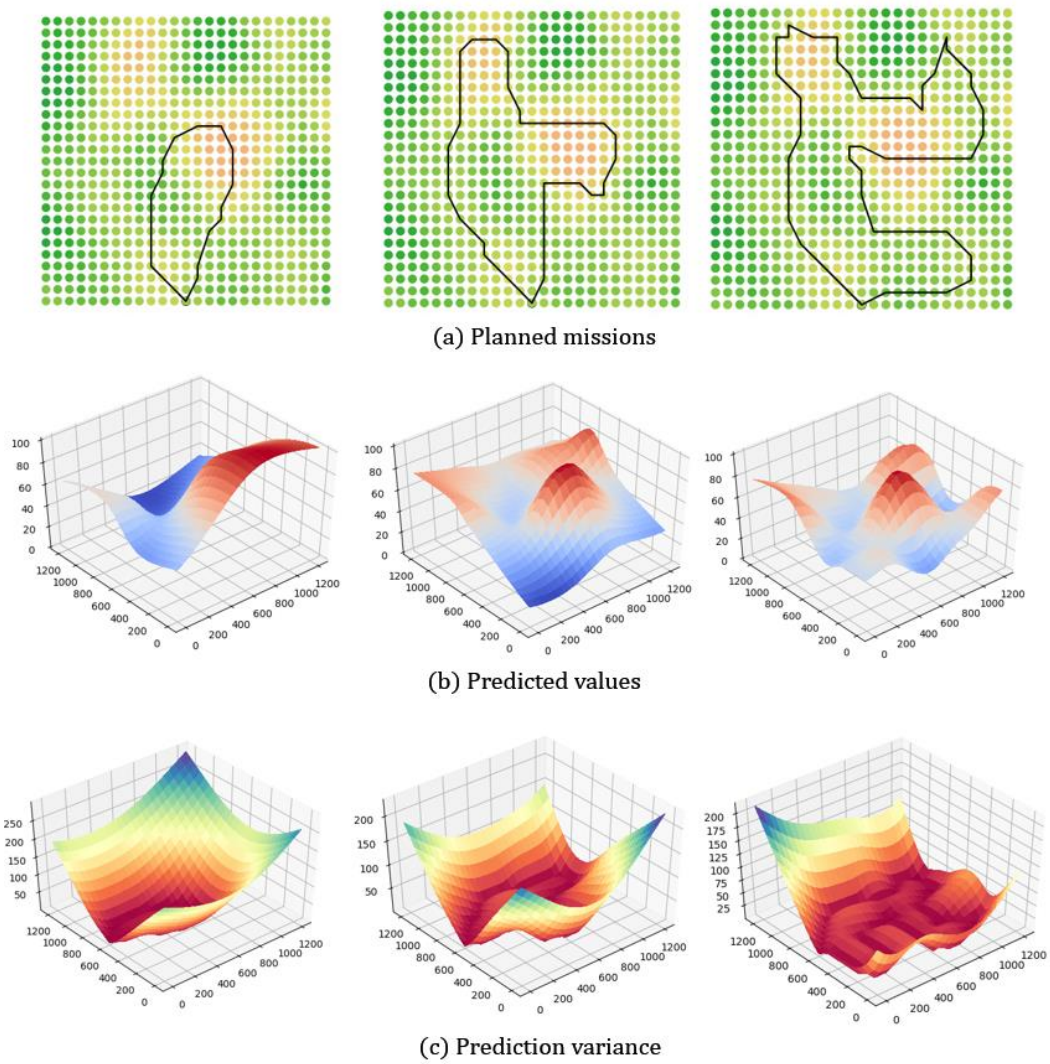

Figure 8: Exemplary comparison of the achieved prediction quality depending on the available flight time. The left-hand column indicates the results obtained for a maximum flight duration of 300 seconds in a representative scenario. The middle and right-hand columns give the results for flight times of 600 and 900 seconds respectively. We indicate (a) the UAV routes, (b) the estimation of the random field achieved by the samples obtained during the flight, and (c) the corresponding prediction error variance across the target area.

Table 2 gives the averaged results for all scenarios evaluated. Obviously, target region size and available flight times have a significant impact on the prediction quality. In particular, shorter flying times correspond to higher prediction errors. However, increasing the available sensing time by a few minutes consistently and significantly improves the information gain achieved. As we have already seen in Figure 8, a flight duration of 1,000 seconds is sufficient to provide a reliable interpolation of the entire target area, i.e. an interpolation associated with small absolute errors and low prediction error variances.

In all scenarios, the average mean error is positive. This is a direct consequence of the prioritization of high-interest targets within the mission-planning algorithm: as targets associated with high values are more likely to be chosen as sensing locations for the UAV, these measurements introduce a positive bias in the interpolation. This also partially explains the higher RMSE. However, we consider this acceptable in an emergency surveillance setting, as information about high-priority targets provides more immediate benefits to a human decision-maker than preventing this biased interpolation.

Table 2: Evaluation of the information gained for different scenarios and maximum flight times. The table indicates average prediction error variance, root-mean-square error (RMSE) and average mean error (ME) for each scenario.

	Flight time [s]	Avg. error variance	Avg. RMSE	Avg. ME
Scenario 1 $(0.75\ \text{km})^2$	300	148.3	31.8	4.2
	600	56.7	17.9	1.1
	900	22.3	7.3	0.8
	1,200	14.7	4.8	0.3
	1,500	5.3	2.9	0.1
	1,800	2.0	2.1	0.2
Scenario 2 $(1\ \text{km})^2$	300	351.6	24.4	6.6
	600	156.5	27.2	4.5
	900	87.9	16.5	2.7
	1,200	48.4	13.2	1.2
	1,500	35.1	9.2	1.0
	1,800	24.1	6.9	0.9
Scenario 3 $(1.25\ \text{km})^2$	300	481.3	39.4	9.4
	600	280.8	37.8	7.7
	900	162.3	28.6	3.0
	1,200	89.0	21.2	1.8
	1,500	68.3	18.9	1.1
	1,800	52.6	18.1	0.9

6 Conclusion and Outlook

In this study, we have presented a mission-planning approach for UAV surveillance flights in the context of firefighting. The vehicles were equipped with remote sensing devices that allow the detection and identification of hazardous substances in smoke clouds. A GIS-based interface allows a member of the emergency response units to specify an area of interest. This tool then plans UAV missions that either guarantee the complete coverage of the target area or focus on a set of high-interest locations if information is required immediately and complete coverage is impossible. The data is streamed live to the base station for further processing. This process, which we call micro rapid mapping, provides spatial data at higher resolutions and with a shorter delay than the Copernicus Rapid Mapping service, which has been proposed for large-scale disasters and is of limited use for many applications in firefighting.

We demonstrate the applicability of this tool using simulated test data representative of real-world use cases. We show that useful initial information can be provided within a few minutes after an incident. If more time is available for the surveillance flight, the mission-planning algorithm is able to increase the area covered significantly. The resulting routes yield reliable information about the underlying spatial phenomenon. In particular, we show that the planning tool is able to balance different objectives, notably ground area covered by a UAV flight as well as priorities within the target area.

Future work should focus on adaptive methods for planning UAV paths in dynamic environments. These methods use the observations made during the flight in order to continuously improve the environmental model that describes the spatial distribution of hazardous substances. UAV missions can then be dynamically adjusted while the flight is still in progress. The methods can thus reduce the dependency on prior information for mission-planning and provide more information in highly dynamic situations.

References

European Parliament (2017). Securing the Copernicus programme. Why EU earth observation matters. Retrieved from: http://copernicus.eu/sites/default/files/library/EPRS_BRI_Copernicus_matters.pdf.

FLIR (2017). FLIR optical gas imaging cameras help to spot gas leaks from the air. Retrieved from: http://www.flir.com/automation/display/?id=70372.

Galceran, E., & Carreras, M. (2013). A survey on coverage path planning for robotics. Robotics and Autonomous Systems, 61(12), pp. 1258-1276.

Gunawan, A., Lau, H. C., & Vansteenwegen, P. (2016). Orienteering problem: A survey of recent variants, solution approaches and applications. European Journal of Operational Research, 255(2), pp. 315-332.

Guzzetti, F., Mondini, A., & Manunta, M. (2012). Mapping and monitoring landslides and ground subsidence. Retrieved from: http://copernicus.eu/sites/default/files/library/SuccessStory_Landslide_and_Subsidence_Winog.pdf.

Lenstra, J., & Kan, A. (1981). Complexity of vehicle routing and scheduling problems. Networks, 11(2), pp. 221-227.

Mulla, D. J. (2013). Twenty five years of remote sensing in precision agriculture: Key advances and remaining knowledge gaps. Biosystems engineering, 114(4), pp. 358-371.

Pebesma, E., Graeler, B., & Pebesma, M. E. (2017). Package 'gstat'. Retrieved from: http://kambing.ui.ac.id/cran/web/packages/gstat/gstat.pdf.

Petrides, P., Kolios, P., Kyrkou, C., Theocharides, T., & Panayiotou, C. (2017). Disaster Prevention and Emergency Response Using Unmanned Aerial Systems. In Stratigea, A., Kyriakides, E., & Nicolaides, C. (Eds.), Smart Cities in the Mediterranean: Springer International Publishing.

Pisinger, D., & Ropke, S. (2007). A general heuristic for vehicle routing problems. Computers & operations research, 34(8), pp. 2403-2435.

QGIS Development Team (2017). QGIS Geographic Information System. Open Source Geospatial Foundation Project. Retrieved from http://qgis.osgeo.org.

Yu, J., Schwager, M., & Rus, D. (2014). Correlated orienteering problem and its application to informative path planning for persistent monitoring tasks. In 2014 IEEE/RSJ International Conference on Intelligent Robots and Systems, pp. 342-349.

Zhang, C., & Kovacs, J. M. (2012). The application of small unmanned aerial systems for precision agriculture: a review. Precision agriculture, 13(6), pp. 693-712.